



Preparation, characterization and comparative ionizing electromagnetic radiation performances: PART II-ceramic reinforced polymeric composites

E. Eren Belgin¹ · G. A. Aycik¹

Received: 20 March 2020 / Accepted: 15 October 2020 / Published online: 29 October 2020
© Akadémiai Kiadó, Budapest, Hungary 2020

Abstract

In this study, isophthalitic unsaturated polyester based composites were prepared by reinforcing with boron carbide, silicon carbide and tungsten carbide. IEMR attenuation properties of the composites were investigated by gamma spectroscopy for different IEMR energies after density evaluation and structural characterization of the composites. Mass attenuation coefficients of composites were higher than lead although they were 5–7 times lighter than lead.

Keywords Ionizing electromagnetic radiation · Radiation shielding · Composite radiation shielding · Polymer composite · Ceramic shielding

Introduction

Ionizing electromagnetic radiation (IEMR) usage became commonplace by the developing technology especially for medical applications for both diagnosis of traumas and several diseases (radiology) and treatment of several diseases (nuclear medicine treatments) especially cancer [1]. Nuclear energy production, industrial and scientific applications are other important usage areas of IEMR. Biological hazards of IEMR were also recognized by the 20th century besides its usage benefits and several shielding materials have been used for protection from these hazards. Especially, chargeless gamma and X-rays with high energy have to be shielded by proper materials because of their high penetrating ability through matter. IEMR interacts with absorber shield's atoms or atomic electrons by transferring its energy while penetrating through the shield material. Thus, energy of IEMR is reduced to acceptable levels or totally depleted. The interaction of IEMR with shielding material increases with high density and closed pack crystal structure of material that increases probability of coming across IEMR with an atom. Lead is traditionally the most widely used shielding

material because of its high density while it has significant disadvantages as toxicity and heaviness.

Due to disadvantages of lead IEMR shielding it became a challenge to develop more convenient composite shielding materials during the last decades. In the literature there are reported studies about polymeric IEMR shielding materials that different polymers are reinforced with different reinforcement materials in this manner.

Tungsten is an excellent substance for attenuating gamma rays due to its high density. However, since tungsten is unstable, it is not available in pure, solid state, therefore, there is difficulty in machining and casting. Thus tungsten or tungsten compound reinforced composite material production studies are carried out by using polymer binders [2, 3]. Nano tungsten reinforced polyethylene [4], tungsten reinforced ethylene vinyl acetate [5], tungsten reinforced epoxy [6] are some of the polymeric composites studied for this purpose.

Boron carbide reinforced composites have been examined mostly in terms of neutron shielding properties in the literature. However, there are also studies on the use of boron reinforcements for gamma shielding in limited numbers. Boron fiber reinforced epoxy matrix [7], composite structures containing paraffin/polyethylene and boron compounds [8], capture thermal neutrons and stop secondary gamma rays using epoxy, amide-polymer and amide-polymer-amine-added boron composites [9], development of composite materials that absorb neutron and gamma rays using steel,

✉ E. Eren Belgin
ebelgin@mu.edu.tr

¹ Chemistry Department, Muğla Sıtkı Koçman University, Kotekli Campus, 48000 Muğla, Turkey

paraffin, polyethylene and boron carbide [8], examination of the neutron and secondary gamma ray attenuation properties of composites containing paraffin and boron carbide [10] are some of these studies.

In another study, where the radiation shielding properties of polymer composites containing tungsten carbide and boron carbide reinforcements were examined together, it was stated that these composites could be a candidate for protection against gamma ray applications [11]. On the other hand, silicon carbide reinforced polymeric composites were not studied as IEMR shielding materials. In addition, in the studies mentioned above, the shielding properties of composites have been studied at different different specific gamma photon energies.

In our previous studies [12–14], as well as first part of this study [15], polymer based composite shielding materials reinforced with metal oxides or minerals are also produced and characterized as alternative IEMR shielding materials. In our previous study [15], isophthalitic unsaturated polyester (PES) based and metal oxide reinforced composites were produced and characterized. Since the produced composites showed good performances, this study was done as continuation of our previous study and unlike the previous study, composites were produced by using ceramic reinforcements (boron carbide (B_4C), silicon carbide (SiC) and tungsten carbide (WC) instead of metal oxides. Thus, in this study it is aimed to investigate effect of ceramic reinforcements on IEMR shielding performances of the composites.

IEMR attenuation properties of the composites were investigated by gamma spectrometric method for different IEMR energies after density evaluation and structural characterization of the composites were held. The IEMR attenuation performance of the ceramic loaded polymer composites has been studied at different specific gamma photon energies (by using relevant radioactive sources/mixed source) in order to understand the possible use of these composites in different areas of their possible application.

Experimental

PES used as composite matrix (1.15 g cm^{-3}) was procured commercially as resin form in styrene monomer. Styrene allowed preparation of a homogeneous mixture by decreasing viscosity of the resin. Commercially procured methyl ethyl ketone peroxide (MEKP) initiator and cobalt octoate (Coct) catalyst were used to carry out polymerization reactions. Three different ceramic reinforcements were used as B_4C , SiC and WC. Commercially procured reinforcements' properties are given in Table 1.

Composites were prepared via radical polymerization reactions by forming crosslinks within PES resin. Details of the production method is given in our previous study [15].

Table 1 Chemical properties of used reinforcements

Reinforcement	Molecular weight (g mol^{-1})	Density (g cm^{-3})	Crystal structure
B_4C	55.255	2.52	Complex
SiC	40.10	3.21	Hexagonal
WC	195.85	15.63	Hexagonal

Table 2 Designations and reinforcement loading ratios of the composites

Reinforcement loading (%)	WC reinforced composites	B_4C reinforced composites	SiC reinforced composites
50	5-WC	5-BC	5-SC
40	4-WC	4-BC	4-SC
30	3-WC	3-BC	3-SC
20	2-WC	2-BC	2-SC
10	1-WC	1-BC	1-SC

Composite designations used in the study and reinforcement loading ratios are given in Table 2.

Densities of the composites were determined experimentally by using an Archimedes' measurement equipment as well as theoretically. Fourier transform infrared spectroscopy (FTIR) analysis were carried out to understand nature of interaction between PES and reinforcements. Scanning electron microscope (SEM) was used for morphological examination of composites. Details of the characterization methods are given in our previous studies [12, 15].

A 110 cm^3 well-type HPGe detector coupled with a 64 k channel analyser and a commercial disc shaped standard mixed point gamma source (Eckert&Ziegler-Mixed) was used for IEMR attenuation performance measurements. Measurements were held for several photopeak energies ranging between 60 and 1836 keV that allows performance examination for low (0–500 keV), intermediate (500–1100 keV) and high (> 1100 keV) IEMR energy regions. The spectra were evaluated by using the Maestro-ORTEC software program and percentage attenuation performances ($F\%$), linear (μ_L) and mass (μ_M) attenuation coefficients of the composites were calculated. Details of the gamma spectrometric measurement set up and methods are given detailed in previous articles [12–15].

Results and discussion

Density and microstructure of the composites

Evaluated experimental and theoretical densities of composites with respect to reinforcement loading ratios are given in Table 3.

As it is seen in Table 3, density of the composites were increased with increasing reinforcement loading ratios, as it was expected, due to higher densities of the reinforcements than composite matrix. The density of the composites were increased approximately 94.7%, 43.6% and 49.6% for 50% loading of WC, B₄C and SiC reinforcements, respectively in proportion of the reinforcement densities. The deviation values of experimental and theoretical densities were ranging between 0.02 and 0.04. Maximum deviation was observed for 5-WC composite with the value of 0.05. These deviation values were thought to be originated from weighting errors that could be done during production and characterization. Thus experimental and theoretical densities of the composites were compatible with each other.

SEM studies were held for polished and fractured surfaces of 50% loaded composites. The SEM micrographs given in Fig. 1 showed that reinforcements were dispersed homogeneously within PES which is the base requirement for production of a proper composite material.

The FTIR spectrums of the 50% reinforced composites and composite matrix PES are given in Fig. 2. The same characteristic transmission bands (~ 1720, 1240, 1015, 790 cm⁻¹) were observed for composite matrix PES and reinforced composites. The insignificant differences between

peak locations of the composites showed that chemical structure of the PES was not change due to reinforcement loading. The bond density of the interested region of analysed sample caused allowable value differences between percentage transmission value of these bands.

IEMR attenuation performances of the composites

F% values of the WC, B₄C and SiC reinforced composites were determined by gamma spectrometry and given in Figs. 3, 4 and 5, respectively.

The predominant interaction process for low (10 keV < *E* < 500 keV) IEMR energy region is photoelectric effect that first falls of rapidly then more slowly with increasing energy for photon energies above the *K*-binding energy of the absorber material. The photoelectric effect is approximately proportional to *Z*⁵ where *Z* represents atomic number of the absorber material. When the IEMR energy rises (600 keV < *E* < 4 MeV) the Compton effect becomes as the process responsible for the energy loss. The Compton scattering per electron is nearly independent of *Z* and therefore the scattering coefficient per atom is proportional to *Z*. The last of the predominant energy loss processes is pair production and it cannot occur when IEMR energy is less than 1.02 MeV. Thus it is the predominant process at high energy region and it is proportional to *Z*² [16].

Thus, an increment tendency of *Z%* values was observed for all the composites as reinforcement loading ratio was increased but accrue of attenuation performance differed as IEMR energy increased due to predominant interaction mechanisms of IEMR with absorber material. Below 500 keV; photoelectric effect and above 1.022 MeV; pair production mechanisms were predominant while Compton scattering is predominant between these energies. The dependency of these mechanisms on atomic number of the absorber were *Z*⁵, *Z* and *Z*² with increasing IEMR energy and according to this phenomenon, the attenuation performances of the composites were expected to show sharpest increment with increasing composite loading ratio for low energies as it is seen in Figs. 3, 4 and 5. The increments were smoother for intermediate IEMR energies while a bit rapid increment were observed at high energies.

Density effect on IEMR attenuation performances of the composites

As it was mentioned before, the composite densities were increased with increasing reinforcement loading ratio since densities of the reinforcements are higher than composite PES matrix. Since density is an important property of a shielding material for both performance and weight, the dependence of *μ_L* values of the prepared composites on densities are shown in Figs. 6, 7 and 8. The mean values

Table 3 Experimental and theoretical densities of the composites

Composite designation	Experimental density (g cm ⁻³)	Theoretical density (g cm ⁻³)	SD
1-WC	1.33	1.27	0.03
2-WC	1.47	1.41	0.03
3-WC	1.65	1.59	0.03
4-WC	1.92	1.83	0.04
5-WC	2.24	2.14	0.05
1-BC	1.28	1.22	0.03
2-BC	1.36	1.29	0.04
3-BC	1.44	1.37	0.03
4-BC	1.54	1.47	0.04
5-BC	1.64	1.58	0.03
1-SC	1.30	1.23	0.04
2-SC	1.38	1.32	0.03
3-SC	1.50	1.42	0.04
4-SC	1.62	1.55	0.04
5-SC	1.72	1.69	0.02

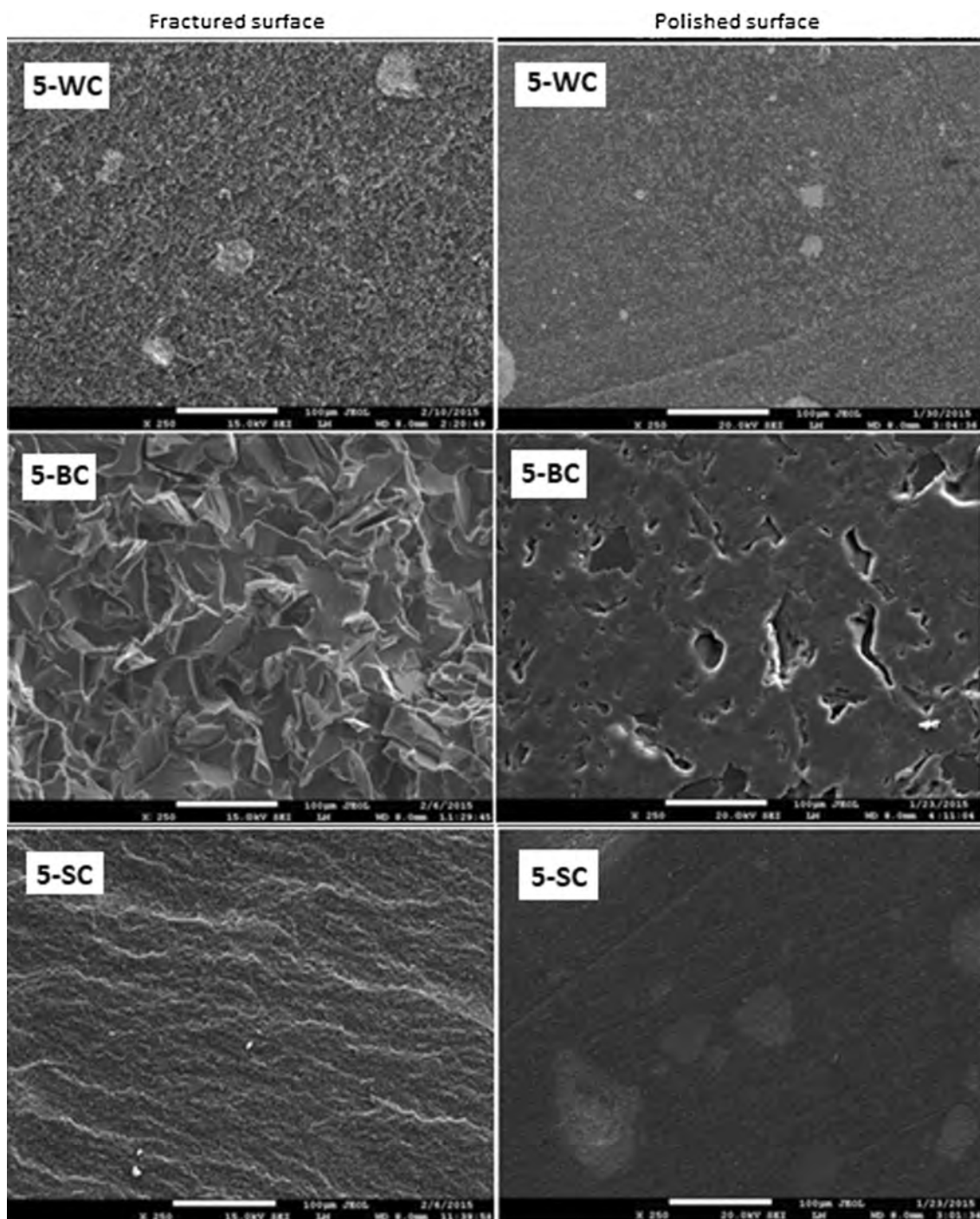


Fig. 1 SEM micrographs ($\times 250$) of polished and fractured surfaces of composites with 50% reinforcement loading ratio

of the IEMR energies subsumed by low, intermediate and high energy regions were used for a more comprehensible comparison. Mean of 60, 122, 166, 392 keV results were taken as low energy result while mean of 662, 898 keV results and mean of 1173, 1333, 1836 keV results were used for intermediate and high energy regions, respectively.

The same phenomenon of different predominant interaction mechanisms for different IEMR energies is manifested itself for μ_L values of composites. In the study, the μ_L values of the composites increased with increasing density of the composites for all energy regions and all composites. This increment was more sharply (due to Z^5 dependence) at low IEMR energy region and the density became less effective on μ_L values for

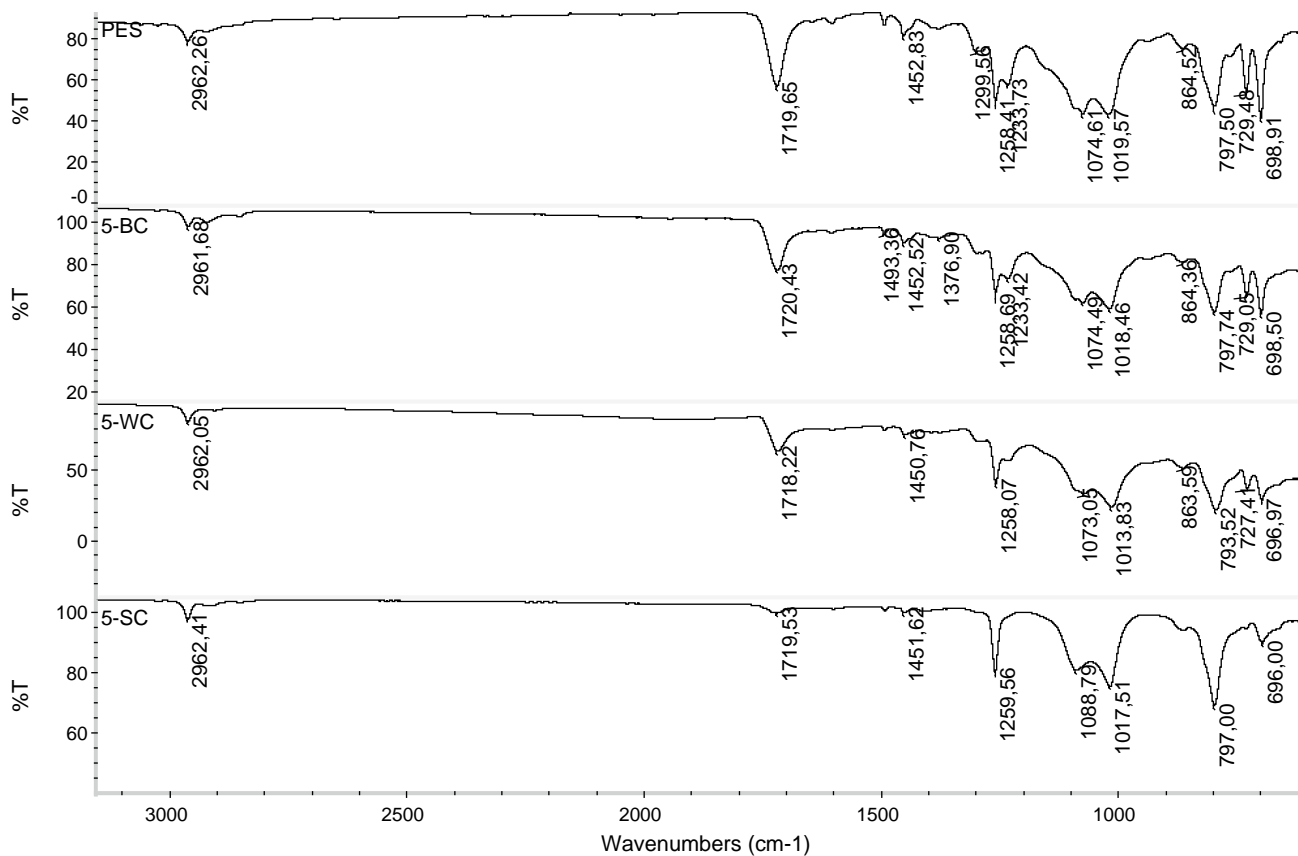
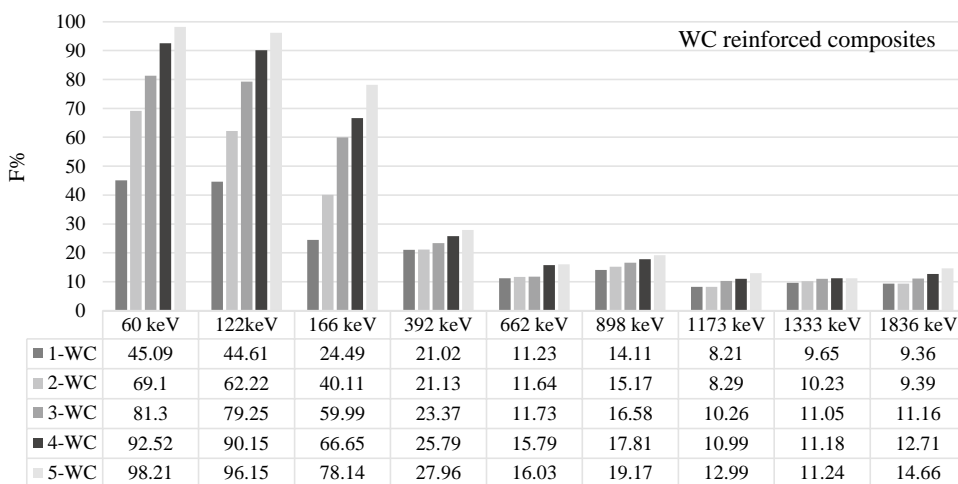


Fig. 2 FTIR spectrums of the PES and 50% reinforced composites

Fig. 3 F% values of WC reinforced composites at different IEMR energies



intermediate (due to Z dependence) energy and high energy (due to Z² dependence) region as it was expected.

Reinforcement type effect on linear and mass attenuation coefficients

IEMR attenuates by the absorber material by interacting with atoms and atomic electrons of the absorber material.

This interaction leads energy loss of the IEMR while penetrating through the material leading low energy at the exit of the material or totally energy lost inside the material. Thus, attenuation of IEMR through the absorber material increases with increasing probability of coming across of IEMR with an atom. This probability increases as density and molecular weight of the absorber material increases. Crystal structure of the material is also a parameter that

Fig. 4 $F\%$ values of B_4C reinforced composites at different IEMR energies

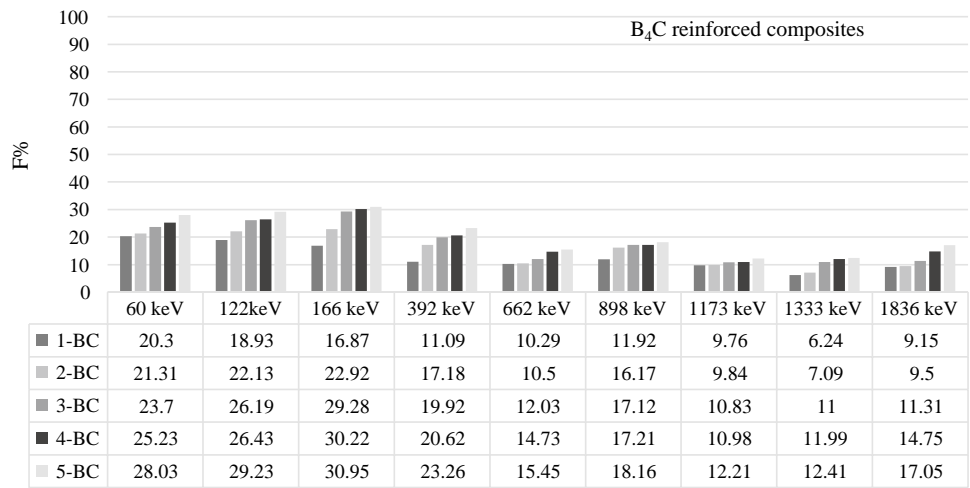


Fig. 5 $F\%$ values of SiC reinforced composites at different IEMR energies

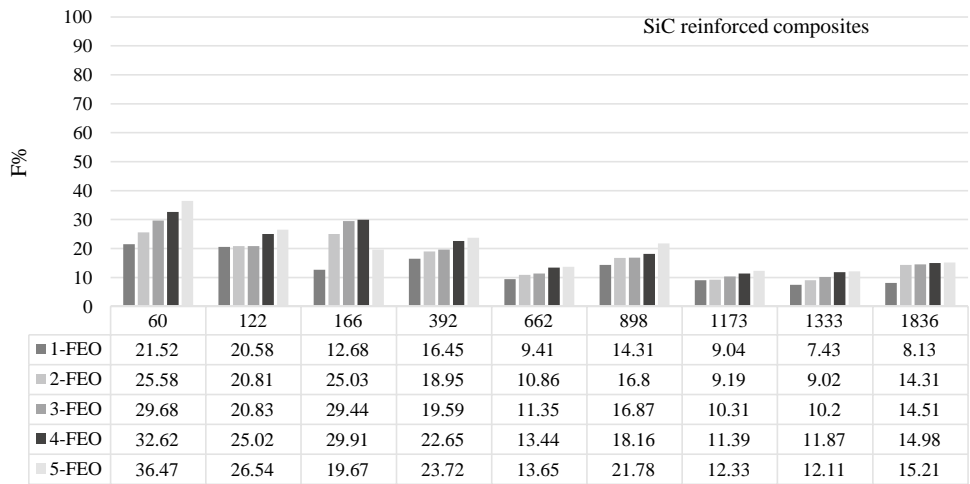


Fig. 6 Plot of dependence of μ_L values on density of WC reinforced composites

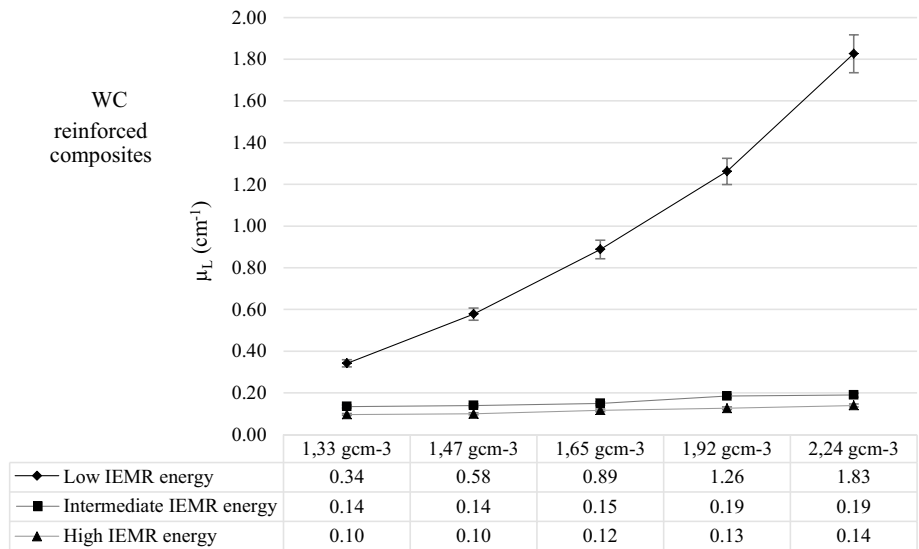


Fig. 7 Plot of dependence of μ_L values on density of B₄C reinforced filled composites

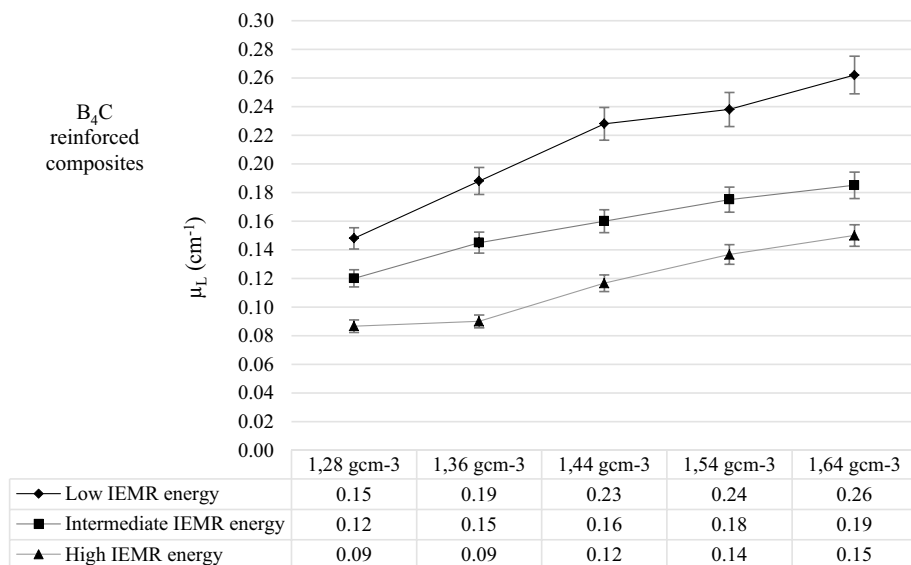


Fig. 8 Plot of dependence of μ_L values on density of SiC reinforced filled composites

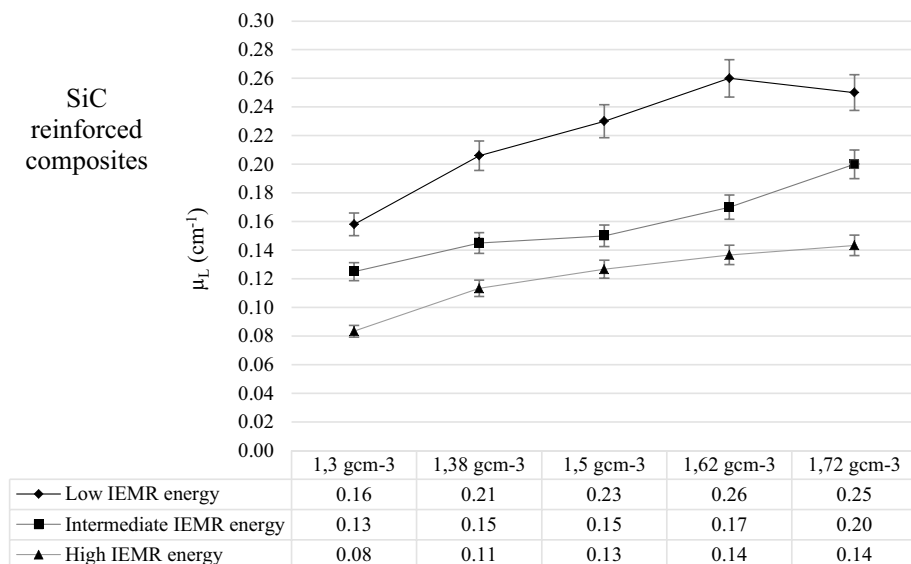


Fig. 9 μ_L values of composites and lead for low, intermediate and high IEMR energy regions

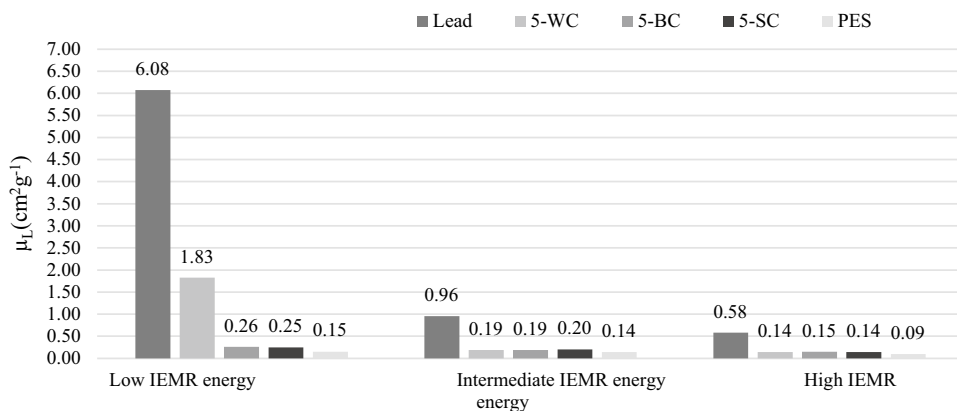
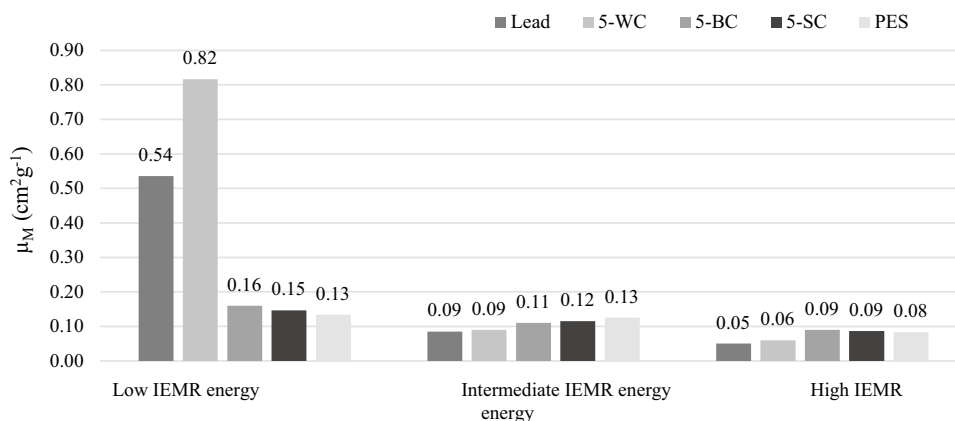


Fig. 10 μ_M values of the prepared composites, PES and elemental lead



effects this probability. If the crystal structure of the material close pack the free volume in the material decreases that increases interaction probability.

In Fig. 9, μ_L values of the 50% reinforced composites (showing the highest performances) and lead are compared for low, intermediate and high energy regions.

In Fig. 9, lead showed higher μ_L values for all energy regions but especially for low IEMR energy region because of the high dependency of attenuation rate on Z number of absorber material at low energies. Lead's high density and closed pack crystal structure makes it a proper IEMR shielding material by high interaction probability of lead atoms with IEMR. On the other hand, the disadvantages of lead as toxicity, heaviness and poor mechanical/chemical properties give rise to novel shielding material pursuit. 5-WC composite reached approximately 30% performance of lead at low energy region. The composites reached approximately 20% and 26% of lead's performance for intermediate and high energy regions, respectively. By fixing our attention on need of light weight shielding materials it was an important point that 5-WC composite was approximately 5.3 times, 5-BC composite was approximately 7.2 times and 5-SC was approximately 6.7 times lighter than lead. Also all the composites was superior when compared to lead due to their non-toxic nature.

In this perspective, not only μ_L value but also μ_M value that gives attenuation performance as unit mass density of the shielding material is an important parameter for a shielding material. Thus μ_M values of the 50% loaded composites, composite matrix PES and lead are given for low, intermediate and high IEMR energy regions in Fig. 10.

As it is seen Fig. 10, although μ_L values of lead was higher than the composites μ_M values of lead was lower than all the composites for intermediate and high energy regions due to its high density. μ_M value of 5-WC composite was also approximately 1.5 times higher than lead for low IEMR energy region.

Conclusions

According to the results, dispersion of reinforcement particles was homogeneous within the PES matrix and chemical structure of the matrix was not changed by reinforcement loading. Different IEMR attenuation performances observed for composites at different energy regions. Composites with higher reinforcement loading showed better attenuation performances. Performance differences became insignificant as IEMR energy increased due to different predominant interaction mechanisms of IEMR with absorber material at different energy levels. Mass attenuation coefficient values of lead was lower than all the composites for intermediate and high energy regions due to its high density. Mass attenuation value of 5-WC composite was also approximately 1.5 times higher than lead for low IEMR energy region. 5-WC composite was approximately 5.3 times, 5-BC composite was approximately 7.2 times and 5-SC was approximately 6.7 times lighter than lead. Also all the composites were superior when compared to lead due to their non-toxic nature.

Acknowledgements The authors would like to acknowledge the financial assistance of the Mugla Sitki Kocman University through the Grant 2014/003 February 2014.

References

1. McCulloch M, Fischer K, Kearfott K (2018) Medical professional radiation dosimeter usage: reasons for noncompliance. *Health Phys* 15(5):646–651
2. Elbatal FH, Ouis MA (2011) UV–visible and infrared absorption spectroscopic studies of gamma irradiated tungsten-doped lithium phosphate glasses. *Phys B* 406:4175–4182
3. Elbatal HA, Abdelghanyb AM, Elbatal FH, Ezzeldinc FM (2012) Gamma ray's interactions with WO_3 -doped lead borate glasses. *Mater Chem Phys* 134:542–548

4. Kim J, Seo D, Lee BC, Seo YS, Miller WH (2014) Nano-W dispersed gamma radiation shielding materials. *Adv Eng Mater* 16:1083–1089
5. Ersoz OA, Lambrecht FY, Soylu HM (2016) Tungsten-ethylene vinyl acetate (EVA) composite as a gamma rays shielding material. *Indian J Pure Appl Phys* 54:793–796
6. Chang L, Zhang Y, Liu Y, Fang J, Luan W, Yang X, Zhang W (2015) Preparation and characterization of tungsten/epoxy composites for gamma-rays radiation shielding. *Nucl Instrum Methods Phys Res B* 356:88–93
7. Bullock RE (1974) Mechanical of a boron-reinforced composite material radiation induced of its epoxy matrix. *J Compos Mater* 8(1):97–101
8. Calzada E, Grünauer F, Schillinger B, Türck H (2011) Reusable shielding material for neutron and gamma radiation. *Nuclear Instruments and Methods in Physics Research A*. 651:77–80
9. Craft AE, King JC (2009) Radiation shielding options for the affordable fission surface power system. In: Robertson GA (ed) CP1103, space, propulsion and energy sciences international forum, SPESIF. American Institute of Physics, College Park
10. Ghassoun J, Senhou N, Jehouani A (2011) Neutron and photon doses in high energy radiotherapy facilities and evaluation of shielding performance by Monte Carlo method. *Ann Nucl Energy* 38:2163–2167
11. Erol A, Pöcan I, Yanbay E, Ersoz OA, Lambrecht FY (2016) Radiation shielding of polymer composite materials with wolfram carbide and boron carbide. *Radiat Protect Environ* 39:3–6
12. Eren Belgin E, Aycık GA (2015) Preparation and radiation attenuation performances of metal oxide filled polyethylene based composites for ionizing electromagnetic radiation shielding applications. *J Radioanal Nucl Chem* 306:107–117
13. Eren Belgin E, Aycik GA, Kalemtaş A, Pelit A, Dilek DA, Kavak MT (2015) Preparation and characterization of a novel ionizing electromagnetic radiation shielding material; hematite filled polyester based composites. *Radiat Phys Chem* 115(43–48):2015
14. Eren Belgin E, Aycik GA, Kalemtaş A, Pelit A, Dilek DA, Kavak MT (2016) Usability of natural titanium-iron oxide as filler material for ionizing electromagnetic radiation shielding composites; preparation, characterization and performance. *J Radioanal Nucl Chem* 309:659–666
15. Eren Belgin E, Aycik GA (2020) Preparation, characterization and comparative ionizing electromagnetic radiation performances: part I—metal oxide reinforced polymeric composites. *J Radioanal Nucl Chem*. <https://doi.org/10.1007/s10967-020-07245-y>
16. Friedlander G, Kennedy JW, Macias ES, Miller JM (1981) *Nuclear and radiochemistry*. Wiley, New York

Publisher's Note Springer Nature remains neutral with regard to jurisdictional claims in published maps and institutional affiliations.